Degradation of benzenesulfonate by heterogeneous photocatalysis combined with ozonation

Zoltán Zsilák,[a] Erzsébet Szabó-Bárdos,[a] Orsolya Fónagy,[a] Ottó Horváth,[*,a]
Krisztián Horváth,[b] Péter Hajós [b]

University of Pannonia, Institute of Chemistry
[a]Department of General and Inorganic Chemistry
[b]Department of Analytical Chemistry
H-8200 Veszprém, POB. 158, Hungary

[*]Corresponding author e-mail: otto@mk.uni-pannon.hu; phone: +36 88 624 159;
fax: +36 88 624 548

Abstract

The efficiency of the photocatalytic degradation of pollutants can be enhanced by combination with another advanced oxidation procedure such as ozonation. Application of these two methods for degradation of benzenesulfonate (BS) resulted in a synergic effect; the efficiency of the combined procedure significantly exceeded the sum of those of the individual techniques. Enhancement of the ozone dosage in this system accelerated the mineralization, i.e., the decrease of the total organic carbon content (TOC), more than the decay (transformation) of BS. The initial rates of both processes displayed a maximum at pH 5-6 in both the aerated and the ozonated systems. An increase of pH in the range of 2-7 promoted the mineralization in the ozonated system more than in the aerated one, while for the decay of BS a reversed relation was observed.
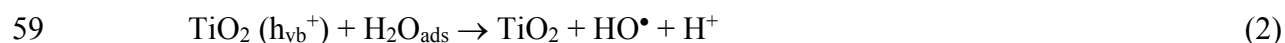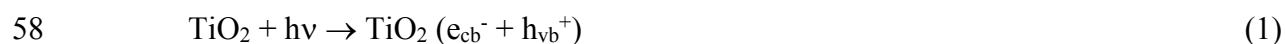
1. Introduction

The use of surface active compounds is widespread in several human activities. Among the anionic surfactants, alkanesulfonates, alkylsulfate, and alkylbenzenesulfonate are

1

commonly applied as cleaning agents, laundry detergents, cosmetics, and personal care products [1].. The extensive use of these compounds leads also to their discharge into the environment, mainly into the water compartment. Linear alkylbenzene sulfonates were thoroughly investigated for their pollution effects and degradation possibilities, but less studies dealt with benzene- and naphthalenesulfonates [2,3]. While the alkyl derivatives were found to be readily biodegradable [4,5], other aromatic sulfonates without long side chains proved to be biorecalcitrant [6]. Biodegradability of benzene- and naphthalenesulfonates with sulfo, nitro and amino groups are especially low [7,8,9]. Due to their strong hydrophilic character (low n-octanol–water partition coefficients [10]), low volatility and high mobility within aquatic systems, polar aromatic sulfonates are easily transported from sewers to surface waters. Hence they are potentially hazardous with respect to contamination of ground water and drinking water supplies [11].

Various methods have been examined for the degradation of these contaminants in the past two decades. Benzenesulfonates was mineralized by contact glow discharge electrolysis [12, 13]. Ozonation was found to be efficient only in the presence of activated carbon, which ensures high local concentration of the reactants through adsorption [14].

Photocatalytic procedures proved to be appropriate for purification of waters contaminated with both inorganic and especially organic pollutants. In heterogeneous photocatalytic methods applied for the degradation of various organic contaminants the most widely used material is titanium dioxide, TiO_2 [3,15,16,17,18,19]. The determining oxidizing species generated in TiO_2-mediated photocatalysis is hydroxyl radical, which is produced in aqueous systems via oxidation of adsorbed water by the positively charged hole (h_{vb}^+) formed in the valence band of the semiconductor upon excitation (Eqs. 1, 2) [20].

$$TiO_2 + h\nu \rightarrow TiO_2 \ (e_{cb}^- + h_{vb}^+) \tag{1}$$

$$TiO_2 \ (h_{vb}^+) + H_2O_{ads} \rightarrow TiO_2 + HO^\bullet + H^+ \tag{2}$$

In air-saturated systems, electrons (e_{cb}^-) photogenerated in the conduction band can reduce dissolved oxygen, leading to the formation of superoxide and peroxide ions (Eqs. 3, 4).

$$TiO_2 \ (e_{cb}^-) + O_{2ads} \rightarrow TiO_2 + O_2^{\bullet-} \tag{3}$$

$$TiO_2 \ (e_{cb}^-) + O_2^{\bullet-} \rightarrow TiO_2 + O_2^{2-} \tag{4}$$

64   Procedures based on TiO$_2$-mediated photocatalysis were successfully applied for

65   degradation of various amino acids [21,22] and surfactants [3,19,23,24,25]. Efficient

66   photocatalytic mineralization of 1,5-naphthalenedisulfonate was also realized in titanium

67   dioxide suspension [26]. In this case, according to a detailed HPLC/MS analysis, the

68   degradation pathway leads to the formation and subsequent decay of benzenesulfonate.

69   Although the photocatalytic degradation of benzenesulfonate was studied in the past

70   [27,28], the possible degradation pathways in this system were just quite recently analyzed

71   [29].

72   Although TiO$_2$ based photocatalysis proved to be an efficient technique for degradation

73   of benzenesulfonate (abbreviated as BS) [29], its combination with another type of advanced

74   oxidation procedure can enhance the efficiency of its mineralization. In this study we

75   demonstrate that ozonation is an appropriate candidate for this purpose. Even if it was

76   successfully applied for degradation of BS only in the presence of activated carbon [14], its

77   combination with heterogeneous photocatalysis results in a synergistic effect in the increase of

78   the mineralization rate. Beside following the total organic carbon (TOC) content of the system

79   treated, monitoring of the concentration of both the starting material (BS) and its hydroxylated

80   derivatives was also carried out. The influence of the ozone dosage and the initial pH on the

81   degradation of BS has also been investigated in order to contribute to the elucidation of this

82   synergy. Beside their theoretical importance, the results of this work can be utilized in the

83   design of new catalytic procedures for wastewater treatment.

84

85   **2. Experimental Section**

86   *2.1. Materials*

87   In all experiments in this study, the titanium dioxide catalyst used was Degussa P25 (70%

88   anatase, 30% rutile; with a surface area of 50 m^2 g^{-1}). The concentration of TiO$_2$ was 1 g dm^{-3}

89   in all cases. Reagent grade benzenesulfonic acid, 4-hydroxybenzenesulfonic acid, and 2,5-

90   dihydroxybenzenesulfonic acid (used as standards for the analyses) were purchased from

91   Merck. Compressed air was bubbled through the reaction mixtures from gas bottles both for

92   stirring and for serving (with its O_2 content) as electron acceptor. Beside dissolved oxygen

93   (O_2), in most of the experiments, O_3 (produced by a LAB2B ozone generator) was also

94   introduced in the same air stream. High purity water applied as solvent in this study was

95   double distilled and then purified with a Milli-Q system.

96

97   ***2.2. Photochemical experiments***

98   Photochemical experiments were carried out in a laboratory-scale reactor with an

99   effective volume of 2.5 dm^3. The heterogeneous reaction mixture (TiO_2 suspension) was

100   circulated by using a peristaltic pump through the reactor and the buffer vessel and by

101   continuously bubbling air with a flow rate of 40 dm^3 h^{-1} within the reactor. The photon flux of

102   the internal light source (40W, λ_{max} = 350 nm, i.e., UVA range) was measured by

103   tris(oxalato)ferrate(III) chemical actinometry [30,31] (I_0 = 4.3×10^{-6} mol photon dm^{-3} s^{-1}).

104

105   ***2.3. Analytical procedures***

106   For analysis, 4 cm^3 samples were taken from the reactors through a septum with a

107   syringe. When the solution part of the sample had to be analyzed, the solid phase was

108   removed by filtration using Millipore Millex-LCR PTFE 0.45 μm filters. The pH of the

109   aqueous phase of the reaction mixture was determined by a SEN Tix 41 electrode.

110   Mineralization was followed by measuring the total organic carbon (TOC) concentration,

111   utilizing a Thermo Electron Corporation TOC TN 1200 apparatus.

112   Benzenesulfonate and its hydroxylated intermediates were followed by HPLC-MS

113   measurements, the conditions of which were described earlier [29]. Sulfate anions were

4

114   analyzed by a Dionex DX300 ion chromatographic system (Dionex, Sunnyvale, CA, USA)

115   using suppressed conductivity detection. The injection volume was 50 μl. Separations were

116   carried out by a Dionex IonPac AS4A-SC (250×4 mm) analytical column. The concentration,

117   pH and flow rate of the carbonate eluent were 3.5 mM, 10.2 and 1.2 ml min^{-1}.

118   The ozone concetration was determined by iodometry, using sodium iodide as reagent

119   and sodium thiosulfate for the titration of the iodine formed.

120

121   ## 3. Results and Discussion

122   ### 3.1. Mineralization of BS under various conditions

123   In order to demonstrate the enhancement in the mineralization rate of BS by application

124   of the combined method ($O_3/TiO_2/UV$), the efficiencies of the simple individual methods

125   were also determined. Fig. 1 displays the change of TOC in systems containing BS of 10^{-3} M

126   initial concentration, during 300-min treatment by ozone alone, together with TiO_2 (in both

127   cases in the dark), as well as UV irradiated O_3, air/TiO_2, and O_3/TiO_2.

128   Insert Fig. 1 about here

129   As the corresponding plots indicate, that the mineralization efficiencies in systems O_3,

130   O_3/TiO_2, and O_3/UV are similar; TOC decreased about 31-32% during the 300-min irradiation

131   period. Apparently, neither TiO_2, nor UV-vis irradiation (here 320 – 420 nm) can significantly

132   affect the oxidation efficiency of ozone. The mineralization rate with irradiated TiO_2 in the

133   presence of dissolved oxygen ($air/TiO_2/UV$) was considerably higher than in the previous

134   cases, demonstrating the much more significant oxidation power of titanium dioxide based

135   photocatalysis. However, combination this method with ozonation ($O_3/TiO_2/UV$) increased

136   the mineralization efficiency much more than the simple addition of the efficiency of O_3 or

137   O_3/TiO_2 would result in. The initial mineralization rates summarized in Table 1 clearly

138 indicate this phenomenon: the initial rate with the combined method (52.9×10^{-2} mg dm^{-3}

139 min^{-1}) is about 1.6 times higher than the sum of the rates observed with the two individual

140 methods (22.9×10^{-2} + 9.8-11.2$\times 10^{-2}$ mg dm^{-3} min^{-1}).

141   Insert Table 1 about here

142 Accordingly, in this case total mineralization was realized within 210-min irradiation.

143   A similar synergistic effect was observed by Li et al [32]. It can be interpreted by the

144 following reactions [33]:

145   -   Direct electron transfer from TiO_2 to O_3:

146       $e_{cb}^- + O_3 \rightarrow O_3^{\bullet-}$ (5)

147       $O_2^{\bullet-} + O_3 \rightarrow O_3^{\bullet-} + O_2$ (6)

148        $O_3^{\bullet-} + H^+ \rightarrow HO_3^{\bullet}$ (7)

149       $HO_3^{\bullet} \rightarrow O_2 + {}^{\bullet}OH$ (8)

150   -   Electron transfer between TiO_2 and O_2 molecule:

151   - $e_{cb}^- + O_2 \rightarrow O_2^{\bullet-}$ (9)

152 The electron scavenging by O_3 or O_2 decreases the possibility of the recombination of the

153 photogenerated electron-hole pair. Besides, formation of very oxidative radicals (e.g., in

154 reactions (6-8)) also enhances the degradation efficiency. Notably, UV irradiation of O_3 may

155 increase the amount of H_2O_2 and HO$^{\bullet}$ species in the system.

156

157 *3.2. Decay of BS and formation of sulfate under various conditions*

6

158   Beside the rate of the mineralization, other quantitative properties of the systems such

159   as the actual concentration of BS and sulfate ions were followed during the irradiations for

160   investigation if the manifestation of synergistic effect can be observed also in the change of

161   these species.

162   Insert Fig. 2 about here

163   A comparison of the initial decay rates of BS with those of the TOC regarding the whole

164   system clearly indicates that in the previous case the rate observed at the combined technique

165   (O_3/TiO$_2$/UV) does not exceed the sum of those of the individual methods (Figs. 1 and 2).

166   This result suggests that the synergistic effect originates from the efficient promotion of the

167   degradation of the intermediates formed during the decay of the starting material (BS).

168   However, as to the rate of the sulfate formation, the increasing effect of the ozonation is much

169   more pronounced, indicating that most of the sulfate ions in this system originated from the

170   intermediates, not from the starting material.

171

172   *3.3. Formation and decay of intermediates in aerated and ozonated systems*

173   The actual concentrations of the starting material (BS) were directly determined from

174   HPLC-MS measurements. Thus, the TOC values corresponding to the unreacted

175   benzenesulfonate could also be calculated. Fig. 3A displays the TOC versus time plots

176   belonging to the overall system, the unreacted surfactant (BS), as well as the intermediates

177   formed during the photocatalytic degradation process in air-saturated system.

178   Insert Fig.3 about here

179   The latter curve is the difference of the previous two. The TOC values corresponding to the

180   intermediates show a maximum at 160-180 min where the concentration of the unreacted

181   benzenesulfonate is still considerable. At longer times (above 180 min) the TOC representing

182   the intermediates is diminishing because the rate of the mineralization of these species

183   exceeds that of their formation. In this period of irradiation, especially above 240 min, the

184   total TOC exclusively belongs to the intermediates because the whole amount of the starting

185   material (BS) has already been transformed. Hence, further decrease of TOC can be attributed

186   to the mineralization of the intermediates. In the presence of ozone (Fig. 3B) the decay of BS,

187   and, thus, the formation of the intermediates is much faster. Accordingly, the corresponding

188   plot shows the maximum TOC value belonging to the intermediates already at about 80 min,

189   and within 120 min all starting BS ions have been transformed. Also the total mineralization

190   took place within 210 min. Since the maximum values of TOC belonging to the intermediates

191   are about the same in both cases (air or ozone), the presence of O_3 accelerates both the

192   formation and the decay of these species.

193

194   ***3.4 The effects of ozone dosage***

195   The experiments with ozonated system, the results of which previously discussed were

196   carried out at constant O_3 dosage (0.12 mM min^{-1}), at less than half of the performance of the

197   ozone generator used. Thus, it was reasonable to investigate how the ozone dosage affects the

198   degradation of BS by using the combined procedure. Fig. 4 displays both the initial rate of the

199   BS decay ($V_0(BS)$) and that of the mineralization, i.e., the TOC decrease ($V_0(TOC)$, as

200   functions of the ozone dosage.

201   Insert Fig. 4 about here

202   It is clearly seen that the increase of $V_0(TOC)$ is steeper than that of $V_0(BS)$ at each value of

203   ozone dozage, and, what is more important, the ratio of these two rates gradually increases

204   upon increasing the O_3 dosage as shown by the data of Table 2.

205   Insert Table 2 about here

206   These data indicate that ozonation promotes the degradation of the intermediates stronger than

207   the transformation (hydroxylation) of the starting material does. A possible explanation of this

208   phenomenon may be that ozonation increases the steady-state concentration of superoxide in

209   this system more than that of the hydoxyl radicals because the latter species alone cannot open

210   the aromatic ring as it was proven in our previous work [29]. Ring-cleavage is an

211   indispensable step for the mineralization of BS .

212   All the three isomers of hydroxy-benzenesulfonate formed and decay during the degradation

213   of BS were followed by HPLC-MS measurements. In the absence of ozone the distribution of

214   the isomers at their maximum (total) concentration is the following: 16% *ortho*, 66 % *meta*,

215   and 18% *para,* in accordance with our earlier results (both theoretical [26] and analytical

216   [29]). Upon ozonation, the percentage of the *o*-hydroxy isomer did not significantly change

217   (14-17%), while that of the *meta* derivative decreased to 51%, with the increase of the *para*

218   species to 32-35 %). Interestingly, the change of the ozone dosage in the range of $0.011 - 0.35$

219   mM min^{-1} did not influence this distribution.

220

221   **3.5. The effects of pH**

222   The pH of this system determines the surface charge of the TiO_2 particles (pH_{zpc} =

223   6.25 [34], and, thus, the adsorption efficiency of the benzenesulfonic acid, which is totally

224   dissociated (pK_{BS} = - 2.36 [14]) in the whole range of pH studied here. Besides, the

225   formations of the reactive oxidizing agents (e.g., $HO^\bullet$, $O_2^{\bullet-}$) as well as their reactions are also

226   affected by pH. Hence, $V_0(BS)$ and $V_0(TOC)$ were also measured as functions of the initial pH

227   (pH_0) in the range of $2.0 - 11.0$, in both aerated and ozonated systems. According to our

228   results shown in Fig. 5, in aerated system the initial rate of both the BS decay and the

229   mineralization display maximum values at about pH 5-6.

230   Insert Fig. 5 about here

231 In the ozonated system the highest $V_0(TOC)$ can be observed at the same pH as in the aerated

232 case, while the maximum of $V_0(BS)$ is a bit lower pH value (ca. 4). These plots indicate that

233 not the adsorption of the determining factor affected by the pH in the range of 2-6, otherwise

234 the initial rate must increase upon acidification, due to the attraction between the positively

235 charged catalyst surface and the anionic benzenesulfonate and their derivatives. Thus, the

236 formation and reaction of the oxidizing agents are the key processes influenced by the pH in

237 these systems. In order to gain more information from these results, the ratios of the initial

238 rates (of both BS decay and TOC decrease) measured in ozonated and aerated photocatalytic

239 systems ($V_0(O_3)/V_0(O_2)$) were plotted as functions of pH_0. As shown in Fig. 6, the

240 transformation of BS is less favored in the ozonated than in the aerated system upon

241 increasing pH values.

242   Insert Fig. 6 about here

243 This phenomenon can be partly attributed to the hindered formation of $HO^\bullet$ radicals from

244 ozone because in these reactions ozonide ions are in protonated form (see reactions (5-8)).

245   On the contrary, for the ratio of the initial rates of mineralization, higher pH values (up

246 to about 7) are more favorable for the ozonated system, which may be explained by the

247 protonation of $O_2^{\bullet-}$, giving $HO_2^\bullet$ being less efficient oxidizing agent than the superoxide

248 radical ($pK(HO_2^\bullet/O_2^{\bullet-}) = 4.8$ [35]). The latter species is the most probable reactant playing key

249 role in the ring-opening, which is indispensable for the mineralization of the aromatic

250 compounds.

251 .

252

253 **4. Conclusions**

254   In this study it has been demonstrated that the combination of titanium dioxide based

255 heterogeneous   photocatalysis   with   ozonation   for   the   oxidative   degradation   of

256 benzenesulfonate results in a synergistic effect, achieving a significantly higher mineralization

257 efficiency than the sum of those of the individual methods. Accordingly, this combination

258 offers an advantageous technique for purification of wastewaters. Since the optimum initial

259 pH for this joint procedure is just slightly acidic (i.e. close to neutral), this condition further

260 promotes the practical application of this combined method.

261

267

268 **Literature Cited**

269

[1] P.S. Tully, In: Grant MH, editor. Kirk-Othmer encyclopedia of chemical technology. 4th ed., vol. 23. New York, JohnWiley & Sons, 1997, p. 194.

[2] F.T. Lange, R. Furrer, H.J. Brauch, Polar aromatic sulfonates and their relevance to waterworks Nieuwegein, Association of River Waterworks – RIWA, 2000, p. 21-60.

[3] A. Rachel, M. Sarakha, M. Subrahmanyam, P. Boule, Applied Catalysis B: Environmental 37(4) (2002) 293.

[4] H. Takada, R. Ishiwatari, Environmental Science and Technology 24(1) (1990) 86.

[5] M.A. Hashim, J. Kulandai, R.S. Hassan, Journal of Chemical Technology and Biotechnology 54(3) (1992) 207.

[6] R.B. Cain, In: Leisinger, T., Cook, A.M., Hutter, R., Nuesch, J.(Eds.), Microbial metabolism of xenobiotics and recalcitrant compounds. Academic Press, London, pp. 325-370.

[7] C. Brilon, W. Beckmann, H.J. Knackmuss, Applied and Environmental Microbiology 42(1) (1981) 44.

[8] D. Zürrer, A.M. Cook, Th. Leisinger, Applied and Environmental Microbiology 53(7) (1987) 1459.

[9] R. Wittich, H.G. Rast, H.J. Knackmuss, Applied and Environmental Microbiology 54(7) (1988) 1842.

[10] H. Greim, J. Ahlers, R. Bias, B. Broecker, H. Hollander, H.P. Gelbke, H.J. Klimisch, I. Mangelsdorf, A. Paetz, N. Schong, G. Stropp, R. Vogel, C. Weber, K. Ziegler-Skylakakis, E. Bayer, Chemosphere 28(12) (1994) 2203.

[11] T. Reemtsma, Journal of Chromatography A 733(1-2) (1996) 473.

[12] R. Amano, S. Tomizawa, M. Tezuka, Electrochemistry 72(12) (2004) 836.

[13] R. Amano, M. Tezuka, Water Research 40(9) (2006) 1857.

[14] P.C.C. Faria, J.J.M. Órfão, M.F.R. Pereira, Applied Catalysis B: Environmental 83(1-2) (2008) 150.

[15] E. Szabó-Bárdos, H. Czili, A. Horváth, Journal of Photochemistry and Photobiology A: Chemistry 154(2-3) (2003) 195.

[16] E. Szabó-Bárdos, H. Czili, K. Megyery-Balog, A. Horváth, Progress in Colloid and Polymer Science 125 (2004) 42.

[17] D. Fabbri, A. Bianco-Prevot, E. Pramauro, Applied Catalysis B: Environmental 62(1-2) (2006) 21.

[18] A. Patsoura, D.I. Kondarides, E.X. Verykios, Catalysis Today 124(3-4) (2007) 94.

[19] S. P. Kamblea, S. B. Sawant, V. G. Pangarkar, Journal of Hazardous Materials 140(1-2) (2007) 149.

[20] M.R. Hoffmann, S.T. Martin, W Choi, W. D.W. Bahnemann, Chemical Reviews 95(1) (1995) 69.

[21] M. Matsushita, T.H. Tran, A.Y. Nosaka, Y. Nosaka, Catalysis Today 120(2) (2007) 240.

[22] E. Szabó-Bárdos, E. Pétervári, V. El-Zein, A. Horváth, Journal of Photochemistry and Photobiology A: Chemistry 184(1-2) (2006) 221.

[23] T. Zhang, T. Oyama, S. Horikoshi, J. Zhao, N. Serpone, H. Hidaka, Applied Catalysis B: Environmental 42(1) (2003) 13.

[24] J. Hegyi, O. Horváth, Progress in Colloid and Polymer Science 125 (2004) 10.

[25] M. Sanchez, M. J. Rivero, I. Ortiz, Applied Catalysis B: Environmental 101(3-4) (2011) 515.

[26] E. Szabó-Bárdos, Z. Zsilák, Gy. Lendvay, O. Horváth, O. Markovics, A. Hoffer, N. Törő, Journal of Physical Chemistry B 112(46) (2008) 14500.

[27] B. Sangchakr, T. Hisanaga, K. Tanaka, K. Journal of Photochemistry and Photobiology A: Chemistry 85(1-2) (1995) 187.

[28] T. Zhang, T. Oyama, S. Horikoshi, J. Zhao, H. Hidaka, N. Serpone, *Solar Energy* 71(5) (2001) 305.

[29] E. Szabó-Bárdos, O. Markovics, O. Horváth, N. Törő, Gy. Kiss, Water Research 45 (2011) 1617.

[30] J.F. Rabek, Experimental methods in photochemistry and photophysics. Wiley-Interscience publication, John Wiley & Sons Ltd., New York, 1982, pp. 944-946.

[31] A.D. Kirk, C. Namasivayam, Analytical Chemistry 55(14) (1983) 2428.

[32] L.Li, W. Zhu, L. Chen, P. Zhang, Z. Chen, Journal of Photochemistry and Photobiology A: Chemistry 175 (2005) 172.

[33] T.E. Agustina, H.M. Ang, V.K. Vareek, Journal of Photochemistry and Photobiology C: Review 6 (2005) 264.

[34] B. Sun, E.P. Reddy, P.G. Smirniotis, Environmental Science and Technology 39 (2005) 6251.

[35] J. Rabani, S. O. Nielson, Journal of Physical Chemistry 73 (1969) 3736.

270   **Figure captions**
271
272   **Fig. 1.** Change of total organic carbon (TOC) content as functions of time in the system
273   containing 1×10^{-3} M BS at $pH_0=3$ during the treatment by various oxidation methods: ($\diamond$) O_3,
274   ($\blacklozenge$) $O_3 +TiO_2$, ($\blacktriangle$) $O_3 + UV$, ($\bullet$) air+TiO_2 + UV, (O) O_3+TiO_2 + UV. (TiO_2 content is 1 g dm^{-3}).

275   **Fig. 2.** Change of the concentration of the starting material (BS) (A) and SO_4^{2-} (B) as functions of
276   time in the system containing 1×10^{-3} M BS at $pH_0=3$ during the treatment by various oxidation
277   methods: ($\blacktriangle$) $O_3 + UV$, ($\bullet$) air+TiO_2 + UV, (O) O_3+TiO_2 + UV. (TiO_2 content is 1 g dm^{-3}).

278   **Fig. 3.** Change of total organic carbon (TOC) content as functions of the irradiation time in the
279   system containing 1×10^{-3} M BS at $pH_0=3$ during the treatment by A) air+TiO_2 + UV and B)
280   O_3+TiO_2 + UV, indicating TOC belonging to the whole system ($\bullet$), the starting material (O), and
281   the intermediates formed ($\blacktriangle$). (TiO_2 content is 1 g dm^{-3}).

282   **Fig. 4.** The initial rate of BS decay ($\bullet$) and mineralization (O) as functions of ozone dosage in the
283   in the system containing 1×10^{-3} M BS at $pH_0=3$, treated by the combined procedure (O_3+TiO_2 +
284   UV). (TiO_2 content is 1 g dm^{-3}).

285   **Fig. 5.** The initial rate of BS decay (A) and mineralization (B) as functions of pH_0 in the system
286   containing 1×10^{-3} M BS, treated by air+TiO_2 + UV ($\bullet$) and O_3+ TiO_2 + UV (O). (TiO_2 content is
287   1 g dm^{-3}).

288   **Fig. 6.** The ratio of the initial rates measured in ozonated and aerated system containing 1×10^{-3} M
289   BS as functions of pH_0, regarding BS decay ($\blacktriangle$) and mineralization ($\triangle$). (TiO_2 content is 1 g
290   dm^{-3}).
291
292

1

293

Table 1. Initial rates of mineralization (i.e., the decrease of TOC) in the system containing 1×10^{-3} M BS at $pH_0=3$ during the treatment by various oxidation methods.

Method	Initial rate / mg dm^{-3} min^{-1}
O_3	10.0×10^{-2}
O_3/TiO_2	9.8×10^{-2}
O_3/UV	11.2×10^{-2}
$Air/TiO_2/UV$	22.9×10^{-2}
$O_3/TiO_2/UV$	52.9×10^{-2}

296
297

Table 2. The ratios of the initial BS decay and mineralization rates at various ozone dosages in the system containing 1×10^{-3} M BS at $pH_0=3$, treated by the combined method ($O_3/TiO_2/UV$).

Ozone dosage (mM min^{-1})	$V_0(TOC)/V_0(BS)$
0	29.8
0.011	30.7
0.016	35.3
0.12	37.5
0.35	44.3

300
301
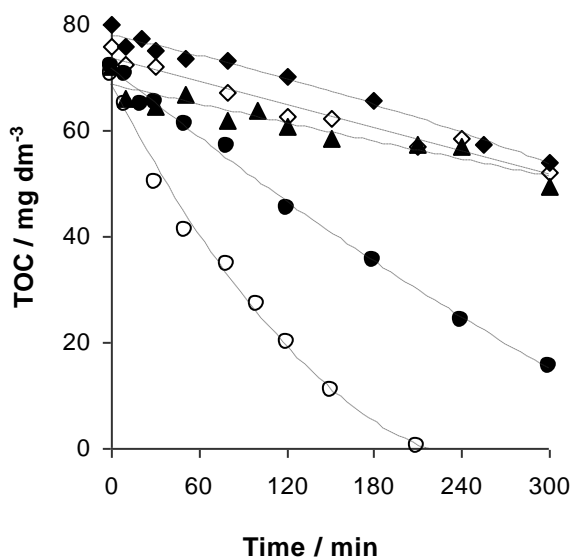
2

302 Fig. 1.

303

312

313

314

315

316 Fig. 2.
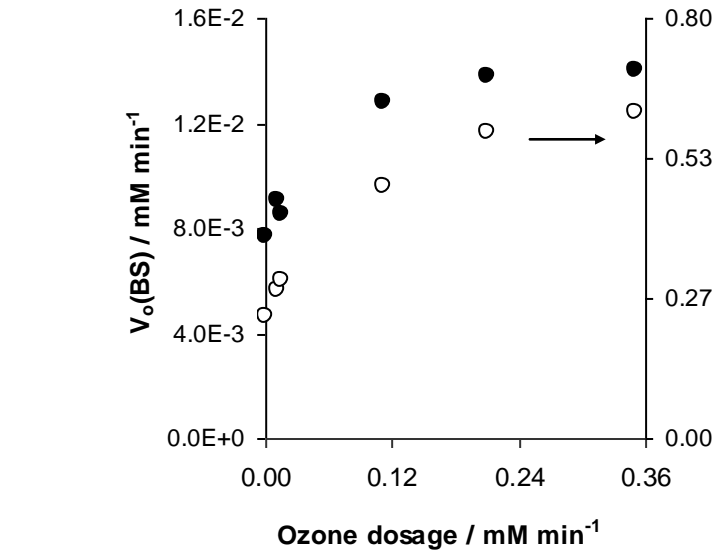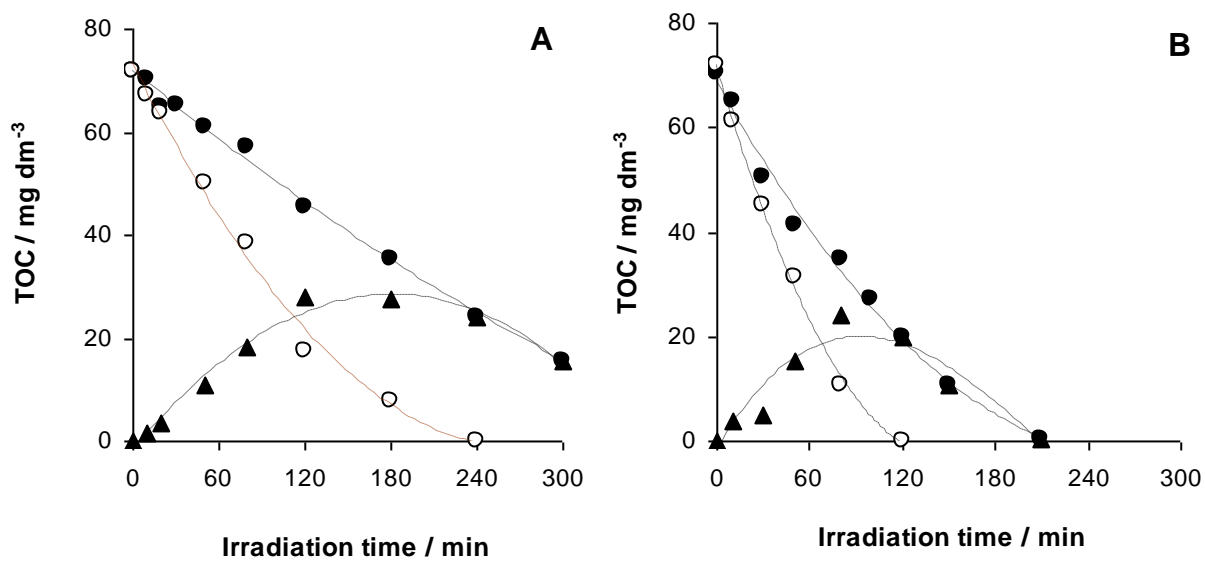
317

327

3

328   Fig. 3.

329

330
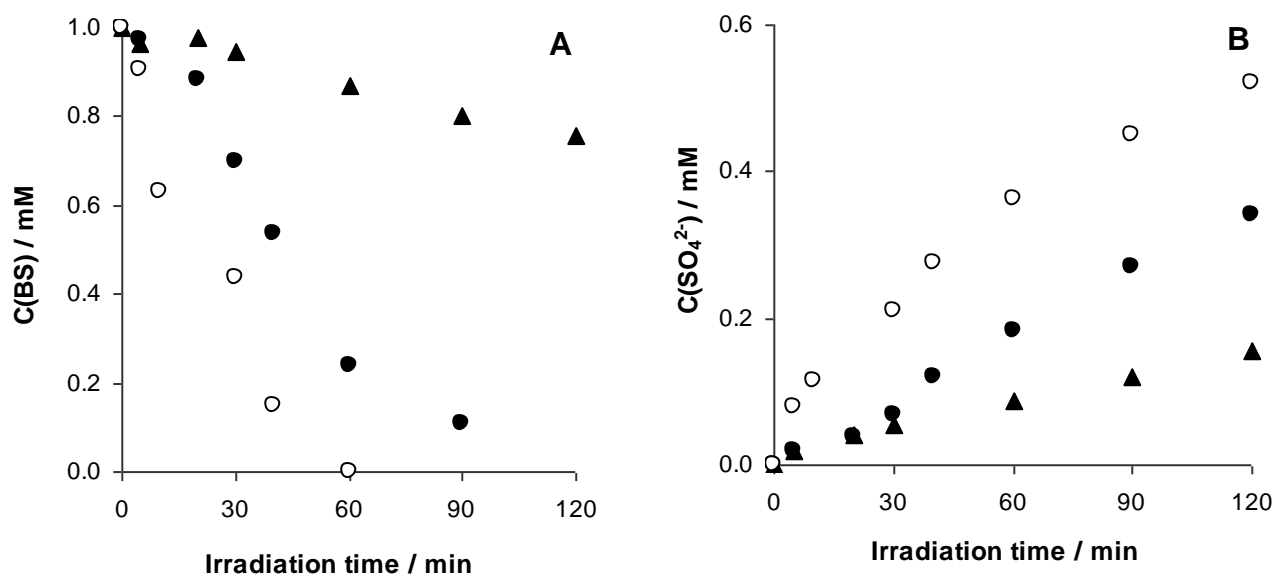
338

339

340

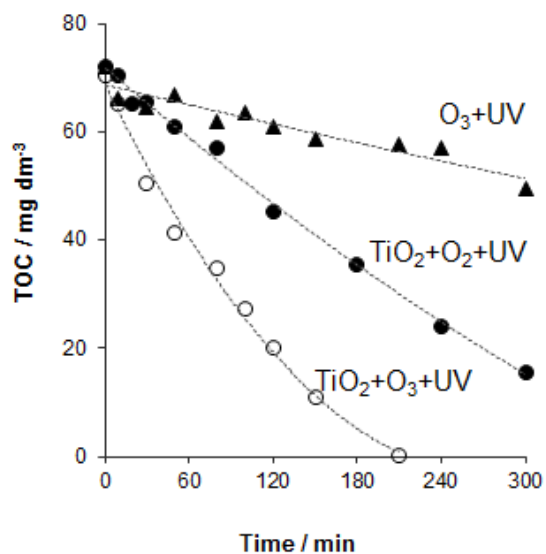341

342   Fig. 4.

343

344

4

345 Fig. 5.

346

357 Fig. 6.

358

359

360

5
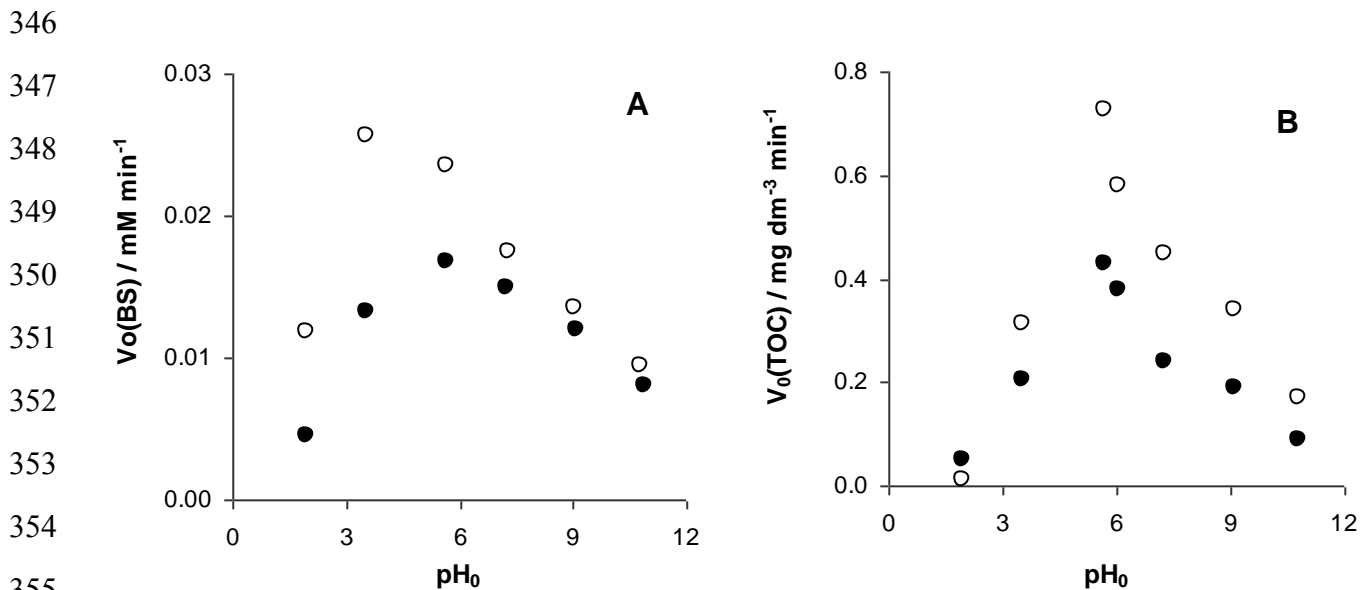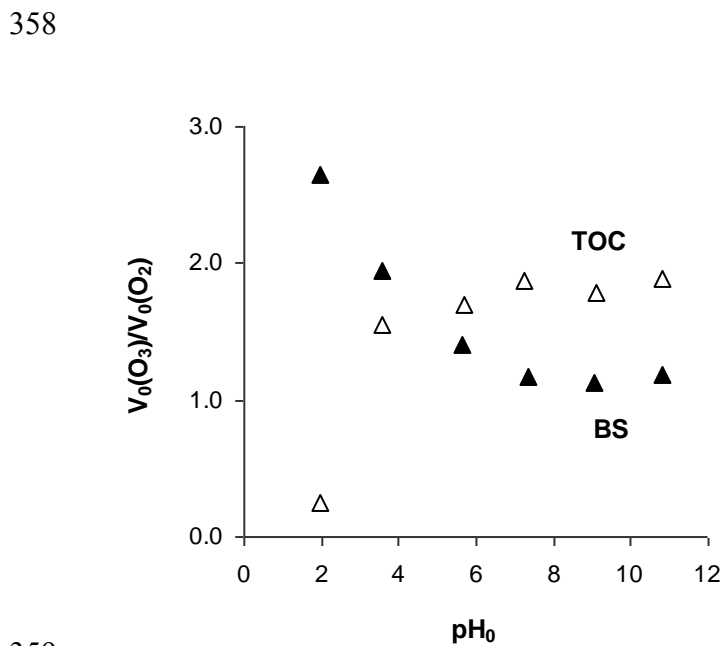
361   Graphical abstract

362

Figure axes: TOC / mg dm^{-3} (y-axis, 0 to 80); Time / min (x-axis, 0 to 300). Curves labeled O$_3$+UV, TiO$_2$+O$_2$+UV, TiO$_2$+O$_3$+UV.

363

364   Application of TiO$_2$ based photocatalysis combined with ozonation for mineralization of
365   benzenesulfonate resulted in synergistic effect, achieving much higher efficiency than the sum of
366   those of the individual methods.

367